

# Finite element failure analysis of continuous prestressed concrete box girders

Zhang Feng<sup>1</sup> Li Shucai<sup>1</sup> Li Shuchen<sup>1</sup> Ye Jianshu<sup>2</sup> Lei Xiao<sup>2</sup>

(<sup>1</sup> School of Civil and Hydraulic Engineering, Shandong University, Jinan 250061, China)

(<sup>2</sup> School of Transportation, Southeast University, Nanjing 210096, China)

**Abstract:** In order to analyze the load carrying capacity of prestressed concrete box girders, failure behaviors of in-situ deteriorated continuous prestressed concrete box girders under loading are experimentally observed and a finite failure analysis method for predicting behaviors of box girders is developed. A degenerated solid shell element is used to simulate box girders and material nonlinearity is considered. Since pre-stressed concrete box girders usually have a large number of curve prestressed tendons, a type of combined element is presented to simulate the prestressed tendons of box girders, and then the number of elements can be significantly reduced. The analytical results are compared with full-scale failure test results. The comparison shows that the presented method can be effectively applied to the failure analysis of in-situ continuous prestressed concrete box girders, and it also shows that the studied old bridge still has enough load carrying capacity.

**Key words:** full-scale failure test; prestressed concrete box girder; finite element analysis; combined element; prestressed tendon; load carrying capacity

A survey of destructive tests of old bridges<sup>[1-2]</sup> reveals that most reinforced concrete bridges possess significant reserve strength despite their already deteriorated conditions, which cannot be predicted by conventional analytical models. In particular, the effects of support conditions and non-structural elements such as the curbs of aged bridges are found to be considerable<sup>[3]</sup>. Even though nonlinear analyses of reinforced concrete structures have shown significant improvements during the past three decades, most efforts in non-linear finite element analysis have focused on simulating the responses of individual elements or simple structural assemblages and verifying the results based on experimental data. Through continued efforts to overcome these limitations, the technique for proper non-linear analysis of complete reinforced concrete frame structures appears to be well established now<sup>[3-4]</sup>. However, full-scale destructive field tests on in-situ bridges focusing on strength and stiffness characteristics of aged reinforced concrete box girders subjected to loading up to failure are rare, and finite element failure analyses focusing on the prestressed concrete box girders are even rarer. In this paper, an in-situ aged prestressed concrete box girder is selected for failure tests and fi-

nite element analysis. In order to effectively simulate the mechanical properties of prestressed tendons, a combined element that can model the straight and curved steel is presented. Finally, finite element failure analysis is performed on the continuous prestressed concrete box girder and obtained responses are compared with the results obtained from the full-scale destructive failure tests.

## 1 Target Bridge

The target bridge for failure analysis and experiments is a continuous prestressed concrete box girder decommissioned for about four years; that is, it is about 15 years old and it was decommissioned in 2005. The old bridge comprises three continuous spans, designed with QCC-20 standard<sup>[5]</sup> with a two-lane roadway. The bridge was decommissioned in 2005 due to cracking at the web of the box girder. The bridge is a three-span continuous structure with a total length of 114 m (32 m + 50 m + 32 m). The longitudinal view of the bridge is shown in Fig. 1. The sections of the prestressed continuous box girder are shown in Fig. 2. In order to ignore the stiffness effect of railings, which is considerable, the railings of the test spans are removed before the test and also ignored in the analysis. Based on standard tests conducted on cores taken from the flanges and the reinforcing bar samples taken from the web, the basic material properties of the bridge are determined. The average values of the measured initial elastic modulus of concrete and the compressive strength are 34 531 and 32.3 MPa, respectively; the yield stress of the reinforcement bar is 200 MPa and that of the prestressed tendon is 1 860 MPa.

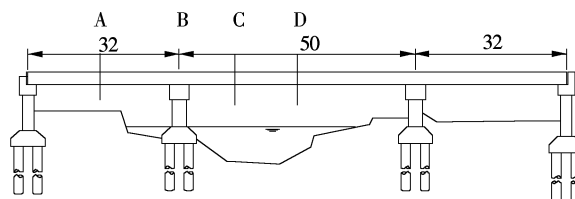


Fig. 1 Longitudinal view of the bridge(unit: m)

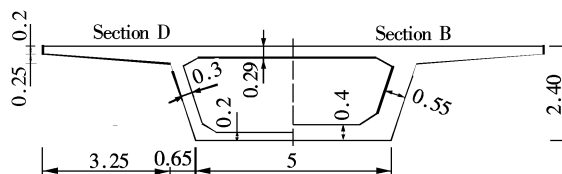


Fig. 2 Cross section of the box girder(unit: m)

Received 2008-11-20.

**Biography:** Zhang Feng (1978—), male, doctor, lecturer, zhangfeng2008@sdu.edu.cn.

**Foundation items:** Post-Doctoral Innovative Projects of Shandong Province (No. 200703072), the National Natural Science Foundation of China (No. 50574053).

**Citation:** Zhang Feng, Li Shucai, Li Shuchen, et al. Finite element failure analysis of continuous prestressed concrete box girders[J]. Journal of Southeast University (English Edition), 2009, 25(2): 236 – 240.

## 2 Failure Tests of Target Bridge

For the target bridge, uniform loading at the mid-span of the interior span is monotonically imposed using steel and

water bags. When the load imposed is around 1 400 t, water is slowly injected into the water bags. A timber bed is used to produce uniform pressure on the flange of the girder. Sensors are installed in the test spans so that measurements can be made to assess the responses of the bridge. Measurements are made at locations where a maximum response is expected. For several locations along the test spans, deflections of girders are measured. The longitudinal strains of the flange concrete and the web concrete are also measured. The target bridge is monotonically loaded in approximately equal increments. The initial values for all applicable response measurements are obtained about an hour before the application of the first load increment. A set of response measurements is made after each load increment.

### 3 Modeling for Failure Analysis of Bridge

Some software<sup>[6-8]</sup> have been used to analyze the steel and concrete structures. Scordelis et al.<sup>[9]</sup> studied the behavior of a skew RC box girder bridge. Ranjit and Abeysinghe<sup>[10]</sup> established a 3D model to assess the capacity and the shear strength of a bridge. Zhou and Zhu<sup>[11]</sup> used the solid degenerate shell element to analyze the load carrying capacity of the box girder. Zhong and Ma<sup>[12]</sup> used the finite segment method to analyze the special box girders. Irawan and Maekawa<sup>[13]</sup> analyzed a box culvert under cyclic loading.

A nonlinear finite element analysis technique is applied to develop a computational technique for failure analysis of aged continuous prestressed concrete box girders, which can effectively predict the relationship between the load and deformation of a three-span continuous prestressed concrete box girder. A layered shell model is used for three-dimensional modeling of concrete and reinforced steel. In-plane constitutive laws of average stress and average strain for concrete in-plane constitutive laws proposed by Hinton and Owen<sup>[14]</sup> are utilized for material modeling. A combined element is used to model the prestressed tendons of the target bridge.

#### 3.1 Constitutive model of concrete

In the model for reinforced concrete, a smeared crack model of concrete is employed by combining the constitutive laws of concrete. The cracked concrete model consists of a tension stiffening model, a compression model and a shear transfer model.

##### 3.1.1 The yield condition of concrete

The yield criterion is formulated in terms of the first two stress invariants, and only two material parameters are involved in its definition.

$$a(q^2) + bp = \sigma_0^2 \quad (1)$$

where  $p = 1/3\text{Tr}(\boldsymbol{\sigma})$ ,  $q = \sqrt{3/2\mathbf{S}:\mathbf{S}}$ ;  $a$  and  $b$  are material parameters, and  $\sigma_0$  is the equivalent effective stress taken as the compressive stress from a uniaxial test. Material parameters can be defined by the uniaxial compression test and the biaxial test under equal compression stresses.

$$a = \frac{1 - 2\bar{f}_{bc}}{\bar{f}_{bc}^2 - 2\bar{f}_{bc}}, \quad b = \frac{1 - \bar{f}_{bc}^2}{\bar{f}_{bc}^2 - 2\bar{f}_{bc}} \sigma_0 \quad (2)$$

where  $\bar{f}_{bc} = f_{bc}/f_c$ ,  $f_c$  is the ultimate uniaxial compressive strength, and  $f_{bc}$  is the ultimate biaxial compressive strength.  $\bar{f}_{bc}$  ranges from 1.16 to 1.2. In this paper, the parameter is 1.16.

##### 3.1.2 Hardening rule

The hardening rule defines the motion of subsequent yield surfaces during plastic deformation. It determines the relationships between the loading surfaces and the accumulated plastic strain. The concepts of effective stress and effective plastic strain make it possible to extrapolate from a simple uniaxial test to a multiaxial situation. In this paper, the relationship between effective stress and effective plastic strain is extrapolated from the uniaxial stress-strain relationship using the follow expression:

$$\sigma = E_0 \varepsilon - \frac{1}{2} \frac{E_0}{\varepsilon_0} \varepsilon^2 \quad (3)$$

where  $E_0$  is the initial elasticity modulus;  $\varepsilon$  is the total strain, and  $\varepsilon_0$  is the total strain at peak stress  $f'_c$ . Inserting the expression  $\varepsilon_c = \sigma/E_0$  in Eq. (3) yields

$$\sigma = -E_0 \varepsilon_p + \sqrt{2E_0^2 \varepsilon_0 \varepsilon_p}, \quad 0.3f'_c < \sigma \leq f'_c \quad (4)$$

where  $\varepsilon_p$  is the plastic strain component, and  $\varepsilon_0$  can be taken equal to  $2f'_c/E_0$  for the normal concrete.

##### 3.1.3 Behavior of steel in tension and compression

The reinforcing bar is considered as steel layers of equivalent thickness or the bar element. A bilinear idealization under repeated loads is adopted in order to model the elastoplastic stress-strain relationships.

#### 3.2 Combined shell element

Some combined concrete steel models have been presented by some scholars. Wu et al.<sup>[15]</sup> proposed a tendon model based on the finite element method that can represent the interaction between tendon and concrete of the prestressed concrete member. Phuvoravan<sup>[16]</sup> presented a new finite element for the nonlinear analysis of reinforced concrete slabs. The connectivity between reinforcement beam elements and the concrete shell element is achieved by means of rigid links.

For modeling the flanges of the box girder of the target bridge, a nine-node degenerated shell element is utilized; the shell element is divided into several layers of panel where the aforementioned constitutive models are applied to each layer of the shell to take into account material non-linearity<sup>[17]</sup>. Each layer is classified as a plain concrete layer or a reinforced concrete layer reached by the bond, so that the cracking behavior is controlled by reinforcing bars being smeared into the layer, as shown in Fig. 3. Since a certain amount of cracked concrete surrounding a reinforcing bar contributes to the stiffness of the element, the whole volume of concrete is considered to contribute to the tension stiffness of the element, so that there is a tension softening effect even inside the plain concrete layer. Each layer contains stress points on its mid-surface. The stress components of the layer are computed at these stress points and are assumed to be constant over the thickness of each layer, so that the actual stress distribution of the shell is modeled by a piecewise

constant approximation. A mid-point interaction rule is applied for each layer.

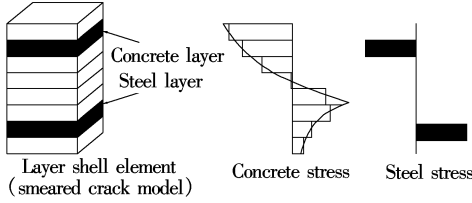


Fig. 3 Layered shell element

Fig. 4 shows the quadratic degenerated shell element that combines bar elements.

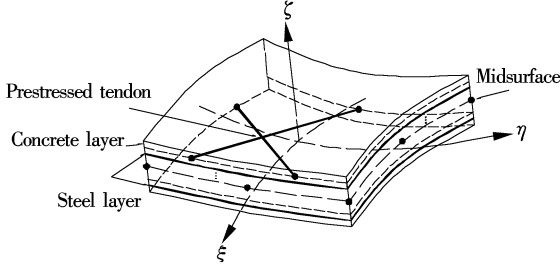


Fig. 4 Proposed element

The displacement vector of the degenerated shell element is

$$\delta_i = \{u_i, v_i, w_i, \beta_{1i}, \beta_{2i}\}^T$$

where  $(u_i, v_i, w_i)$  is the displacement of the node in the global coordinate system;  $(\beta_{1i}, \beta_{2i})$  is the rotation of the node in the nodal coordinate system.

The internal force vector is

$$F_i = \{f_{ui}, f_{vi}, f_{wi}, M_{1i}, M_{2i}\}^T$$

Then the element displacement field can be expressed as

$$u = \sum_{k=1}^n N_k u_k^{\text{mid}} + \sum_{k=1}^n N_k \frac{h_k}{2} \zeta (-v_{2k}^x \beta_{1k} + v_{1k}^x \beta_{2k})$$

$$v = \sum_{k=1}^n N_k v_k^{\text{mid}} + \sum_{k=1}^n N_k \frac{h_k}{2} \zeta (-v_{2k}^y \beta_{1k} + v_{1k}^y \beta_{2k})$$

$$w = \sum_{k=1}^n N_k w_k^{\text{mid}} + \sum_{k=1}^n N_k \frac{h_k}{2} \zeta (-v_{2k}^z \beta_{1k} + v_{1k}^z \beta_{2k})$$

where  $n$  is the number of the nodes per element;  $N_k$  is the element shape function.  $h_k$  is the shell thickness at node  $k$ .  $u_k^{\text{mid}}, v_k^{\text{mid}}, w_k^{\text{mid}}$  are the displacements of node  $k$  in the global coordinate set at the mid surface of the degenerate shell element.  $v_{1k}^x, v_{1k}^y, v_{1k}^z$  are the  $x$  value's projection of the nodal coordination system to the global coordination system.  $v_{2k}^x, v_{2k}^y, v_{2k}^z$  are the  $y$  value's projection of the nodal coordination system to the global coordination system.

The displacements of the nodes of steel are grouped in the following vector:

$$\delta_s = \{u_a, v_a, w_a, u_b, v_b, w_b\}^T$$

where  $u_a, v_a, w_a$  are the displacements of one node of bar elements;  $u_b, v_b, w_b$  are the displacements of another node of

bar elements.

The displacements of the nodes of shell elements are grouped in the following vector:

$$\delta_c = \{\delta_{c1}, \delta_{c2}, \dots, \delta_{c9}\}^T$$

where  $\delta_{ck} = \{u_k^{\text{mid}}, v_k^{\text{mid}}, w_k^{\text{mid}}, \beta_{1k}, \beta_{2k}\}$ ,  $k = 1, 2, \dots, 9$ .

The nodal displacement relationship between the degenerate shell element and the steel is

$$\delta_s = [R_1 \quad \dots \quad R_9] R \delta_c \quad (5)$$

where

$$R_k = \begin{bmatrix} N_1 & N_1 \frac{h_k}{2} \zeta_a v_{1k}^x & -N_1 \frac{h_k}{2} \zeta_a v_{2k}^x \\ N_1 & N_1 \frac{h_k}{2} \zeta_a v_{1k}^y & -N_1 \frac{h_k}{2} \zeta_a v_{2k}^y \\ N_1 & N_1 \frac{h_k}{2} \zeta_a v_{1k}^z & -N_1 \frac{h_k}{2} \zeta_a v_{2k}^z \\ N_2 & N_2 \frac{h_k}{2} \zeta_b v_{1k}^x & -N_2 \frac{h_k}{2} \zeta_b v_{2k}^x \\ N_2 & N_2 \frac{h_k}{2} \zeta_b v_{1k}^y & -N_2 \frac{h_k}{2} \zeta_b v_{2k}^y \\ N_2 & N_2 \frac{h_k}{2} \zeta_b v_{1k}^z & -N_2 \frac{h_k}{2} \zeta_b v_{2k}^z \end{bmatrix}$$

$$N_1 = N_k(\xi_a, \eta_a), \quad N_2 = N_k(\xi_b, \eta_b)$$

where  $R$  is called the transformation matrix that defines the relationship between the displacement of the bar element and that of the solid degenerated shell element.

The stiffness contribution of the steel to the combined element can be written as

$$K_{sc} = R^T K_s R \quad (6)$$

where  $K_s$  is the stiffness matrix of steel.

The stiffness of the combined element is the sum of the stiffness of the solid degenerated shell  $K_c$  and stiffness contribution of the steel to the combined element  $K_{sc}$ .

$$K = K_c + K_{sc} \quad (7)$$

### 3.3 Finite element modeling

A finite element model of the target bridge is established. The solid degenerated shell element is used to model the flanges of the box girder. The layer model is used and the shell element is divided into 10 layers. The total number of elements is 580. Prestressed tendons at the webs of box girders are modeled by combined elements. Prestressed tendons at the top flange and the bottom flange are modeled by a layered model. Fig. 5 shows the details of the finite element modeling of the target bridge.

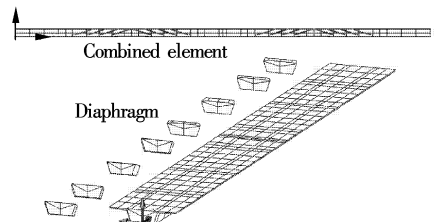


Fig. 5 Finite element model

4 Failure Analysis and Comparisons

Fig. 6 and Fig. 7 show vertical displacement comparisons between the experimental results and the computed results. The response of the target bridge up to a load of about 5 MN is almost elastic. It is shown that the computed ultimate load on the box girder reaches 17.160 MN, which is lower than the capacity obtained from the destructive test (18.678 MN). It is found that the target bridge possesses a higher strength than the theoretical ultimate strength. The obtained maximum load is 1.29 times higher than the ultimate load of 14.435 MN computed analytically according to Chinese code<sup>[5]</sup>. It is known that the code analysis leads to conservative predictions of bridge capacity. One possible reason can be that the material strength of concrete reinforcing bars in-situ is usually much greater than the specified nominal values used in design. Considering this difference, the material properties of the target bridge are measured from concrete cores and reinforcing bars taken from the bridge used in the analysis.

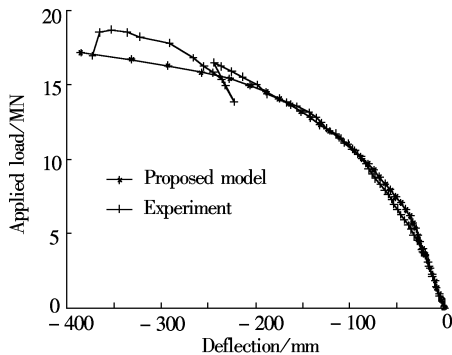


Fig. 6 Load-deflection curve at section D

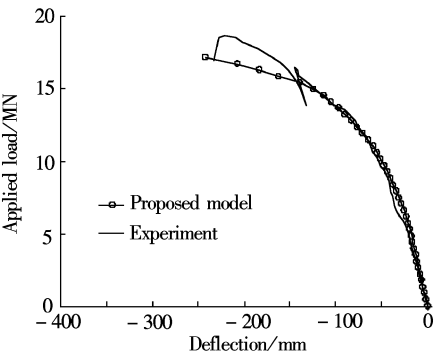


Fig. 7 Load-deflection curve at section C

The comparison of normal stresses of concrete is shown in Fig. 8. Fig. 8 shows that the maximum normal stress of concrete is about -25 MPa which is at the bottom flange at section B. The computed results are in agreement with the experimental results.

Fig. 9 shows load-stress responses of prestressed tendons. The prestressed tendon at the bottom flange at section D is similar to yield and its stress is 1548 MPa, and its stress increases quickly after box girder cracking. The stresses of prestressed tendons at other positions are relatively low.

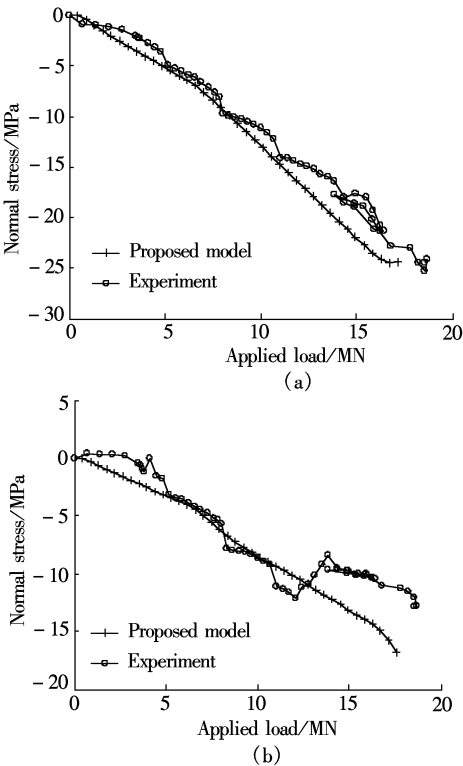


Fig. 8 Comparison of normal stress of concrete. (a) Bottom flange at section B; (b) Top flange at section D

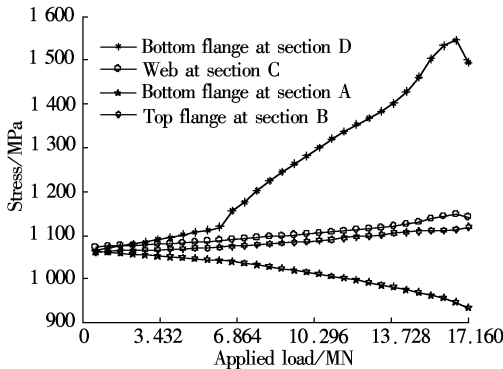


Fig. 9 Stress of prestressed tendon

5 Conclusion

For a three-span prestressed continuous box girder, full-scale destructive tests have been performed by applying loads up to failure to observe the failure behaviors of the bridge experimentally and finite element analyses have been carried out to predict its behaviors analytically. Experimental results indicate that significant load carrying capacity is retained in the old prestressed concrete box girder. In order to effectively simulate the mechanical properties of prestressed tendons, a combined element that can model straight and curve steel is presented. The element can model all kinds of steel disposal fashions and it describes the mechanical properties of the steel and the concrete expediently. By using this method, the number of elements is significantly reduced. Analytical results and comparisons with the experimental results show that the finite element analysis technique proposed in this paper can be effectively applied to the failure analysis of in-situ prestressed concrete continuous box girders.

## References

- [1] Bakht B, Jaeger L G. Bridge testing—a surprise every time [J]. *J Struct Eng*, 1990, **116**(5): 1370–1383.
- [2] Huria V, Lee K-L, Aktan A E. Nonlinear finite element analysis of RC slab bridge[J]. *J Struct Eng*, 1992, **119**(1): 88–107.
- [3] Ho I, Shahrooz B M. Finite element modeling of a deteriorated R. C. slab bridge: lessons learned and recommendation [J]. *Struct Eng Mech*, 1998, **6**(3): 259–274.
- [4] Okamura H, Maekawa K. *Nonlinear analysis and constitutive model in reinforced concrete* [M]. Tokyo: Gihodo-Shuppan Co., 1991.
- [5] Ministry of Transport of China. JTG D60—2004 General code for highway bridges and culverts [S]. Beijing: China Communications Press, 2004. (in Chinese)
- [6] Park Y J. IDARC: inelastic analysis of reinforced concrete frame shell wall structure[R]. New York: University at Buffalo, the State University of New York, 1987.
- [7] Li Kangning. CANNY: a computer program for 3D nonlinear dynamic analysis of building structures [R]. Singapore: National University of Singapore, 1993.
- [8] Maekwaw K, Pimanmas A, Okamura H. *Nonlinear mechanics of reinforced concrete* [M]. Oxford, UK: Taylor and Francis Press, 2003.
- [9] Scordelis A C, Boukamp J G, Wasti S T, et al. Ultimate strength of skew RC box girder bridge [J]. *Journal of the Structural Division*, 1982, **108**(ST1): 105–121.
- [10] Ranjit S, Abeysinghe M. Pushover analysis of inelastic seismic behavior of Greveniotikos bridge [J]. *Bridge Engrg*, 2002, **7**(2): 115–126.
- [11] Zhou Shijun, Zhu Xi. Nonlinear finite element analysis and model tests of reinforced concrete box girders [J]. *China Civil Engineering Journal*, 1996, **29**(4): 21–29. (in Chinese)
- [12] Zhong Xingu, Ma Ping. Nonlinear finite element analysis of thin-walled multicell box girder [J]. *China Civil Engineering Journal*, 1999, **32**(6): 32–39. (in Chinese)
- [13] Irawan P, Maekawa K. Path-dependent non-linear analysis of reinforced concrete shells [J]. *Journal of Material, Concrete Structures and Pavements*, 1995, **17**(2): 1263–1268.
- [14] Hinton E, Owen D R J. *Finite element software for plate and shells* [M]. Swansea: Pineridge Press, 1984.
- [15] Wu X H, Otani S, Shiohara H. Tendon model for nonlinear analysis of prestressed concrete structures [J]. *Journal of Structural Engineering*, 2001, **27**(4): 398–405.
- [16] Phuvoravan K. Nonlinear finite element for reinforced concrete slabs [J]. *Journal of Structural Engineering*, 2005, **131**(4): 643–649.
- [17] Irawan P. Three dimensional analysis of reinforced concrete structures [D]. Tokyo: University of Tokyo, 1995.

## 预应力混凝土连续箱梁有限元损伤分析

张 峰<sup>1</sup> 李术才<sup>1</sup> 李树忱<sup>1</sup> 叶见曙<sup>2</sup> 雷 笑<sup>2</sup>

(<sup>1</sup>山东大学土建与水利学院, 济南 250061)

(<sup>2</sup>东南大学交通学院, 南京 210096)

**摘要:**为了确定预应力混凝土箱梁的极限承载能力,进行了预应力混凝土连续箱梁的破坏性试验,提出一种有限元损伤分析方法模拟箱梁结构行为.基于实体退化壳单元对箱梁进行模拟,并考虑了结构材料的非线性效应.由于预应力混凝土箱梁中通常存在大量曲线预应力钢筋,提出一种组合单元,并用该单元模拟箱梁中的预应力钢筋,该方法可使结构分析时单元数量大大降低.试验结果和理论分析对比表明:提出的方法能够有效地用于预应力混凝土连续箱梁的破坏性试验计算分析中;研究的旧桥依然存在较大的极限承载能力.

**关键词:**实桥破坏性试验;预应力混凝土箱梁;有限元分析;组合单元;预应力钢筋;极限承载能力

**中图分类号:**U448.35